# Synthesis and characterizations of (Bi0.5Na0.5)TiO3-LiNbO3 ceramic system

**This thesis is submitted in partial fulfilment of the requirement for the degree of**

**Master of Science in**

**PHYSICS**

**By**

**BIJENDRA JYOTISH**

**Under the supervision of**

**Prof. S. Panigrahi**

**DEPARTMENT OF PHYSICS**

**NATIONAL INSTITUTE OF TECHNOLOGY, ROURKELA**

**2012-2013**

**NATIONAL INSTITUTE OF TECHNOLOGY**
**ROURKELA**

# CERTIFICATE

This is to certify that the thesis entitled "**Synthesis and characterization of $Bi_{0.5}Na_{0.5}TiO_3 - LiNbO_3$ ceramic system**" submitted by Bijendra Jyotish in partial fulfilments for the requirements for the award of the degree in Master of Science in Physics, National Institute of Technology, Rourkela is an authentic work carried out by him under my supervision and guidance.

To the best of my knowledge, the matter embodied in this project has not been Submitted to any other University/ Institute for the award of any degree in M.Sc Physics.

**Place: Rourkela**
**Date: 07.05.2013**

**Prof. S. Panigrahi**
**Dept. of Physics**
**National Institute of Technology**
**Rourkela-769008**

# ACKNOWLEDGEMENT

First of all I express my appreciativeness to Prof. S.Panigrahi for his support, valuable expert guidance rendered to me and his acceptance of me as a M.Sc student working under his guidance. I am especially indebted to PhD scholars BiswanathParija, RakeshMuduli, Priyambada Nayak and Ranjit Pattnaik for their valuable suggestions and clarifying all my doubts.

I also express my thankfulness to PhD scholar BiswanathParija for helping me in completing my project and analysing the data.

Lastly but not the least I would like to express my gratefulness to my parents and my brother for their endless support without which I could not have completed my project work.

07.05.2013 BIJENDRA JYOTISH

DEDICATED
TO
MY PARENTS

## ABSTRACT

Lead free (1-*x*)(Bi0.5Na0.5)TiO3–*x*$LiNbO_3$ ceramics were prepared by solid state reaction route taking five different compositions with x = 0.02, 0.04, 0.06,0.08 and 0.10. From XRD pattern it is confirmed that the BNT-LN single phases were formed at different LiNbO3 doping. The RAMAN pattern shows roughness or irregularity due to the data taken at high resolution. From morphological study by SEM it is found that the grains were well developed and have the dense structure. Also the grain shape changes from granular to platted with increase in concentration of LINbO3. From UV-VIS SPECTROSCOPY it is observed that the band gap increases with increase in LiNbO3 concentration. The PE-LOOP analysis shows that the remnant polarization (Pr) and coercive field (Ec) values increase with increase in concentration. The dielectric study shows that the dielectric constant increases with increase in temperature also the broadening of the peaks is observed with increase in concentration

**CONTENTS** **PAGE NO**

# CHAPTER-1

## INTRODUCTION

Dielectrics are basically electric insulators. In such materials the electrons are very tightly bound to the atoms and they do not conduct any electric current. In dielectrics the centers of positive and negative charges coincides. So no conductivity is possible. When a sufficient magnitude of electric field is applied to the crystal the centres of positive charges slightly displaced in the direction of field and the negative charges in opposite direction. This produces electric dipoles throughout the crystal. And the crystal is said to be polarized.

Examples of dielectrics are : glass, porcelain, pure water, methyl chloride($CH_3Cl$), hydrogen, nitrogen, ammonia($NH_3$)

## POLARIZATION

When a dielectric material is placed in an external electric field , it becomes polarized i.e. in a small volume of substance the geometrical sum of the electric dipole moment vectors of the molecules becomes nonzero.

The polarization P is expressed as the dipole moment per unit volume

$$\text{i.e. } P = p / v$$

If N be the number of molecules per unit volume and if each has a moment p then the polarization is given by

$$P = N*p$$

## FREQUENCY DEPENDENCE OF POLARIZATION

The electric polarizability of the atom is defined as the dipole moment per local electric field

$$\text{i.e. } \alpha = p/E_{loc}$$

The net polarizability (α) of a dielectric material results mainly from four contributions and these are:-

i. Space charge polarizability
ii. Dipolar polarizability
iii. Electronic polarizability
iv. Ionic polarizability

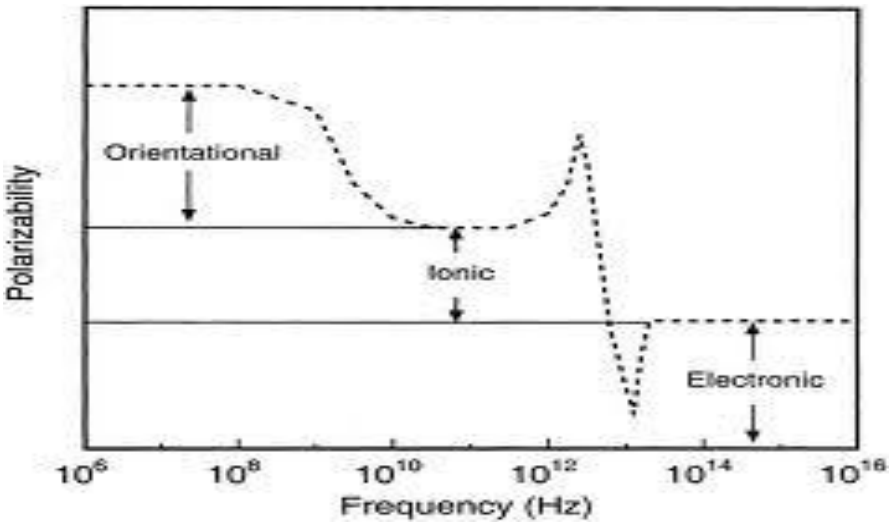


**Fig.1-Graph Showing the variation of polarizability w.r.t Frequency**

At lower frequency all kind of polarization takes place. But as we increase the frequency, slowly the polarizations filters out and in optical frequency range the dielectric constant arises almost entirely from the electronic polarization.

## CLASSIFICATION OF SYMMETRY CLASSES(POINT GROUPS)

There are 32 symmetry classes (point groups) out of which 21 point groups are non-centrosymmetric and 11 are having center of symmetry. We are interested in these 21 groups as they possess dipoles. Again out of 21, 20 groups show piezoelectric behaviour. Out of these 20 point groups, 10 point groups have unique Polar axis (i.e. polarizes with the application of electric field) and are exhibit pyroelectric effect. These 10 divided into ferroelectrics and non-ferroelectrics.

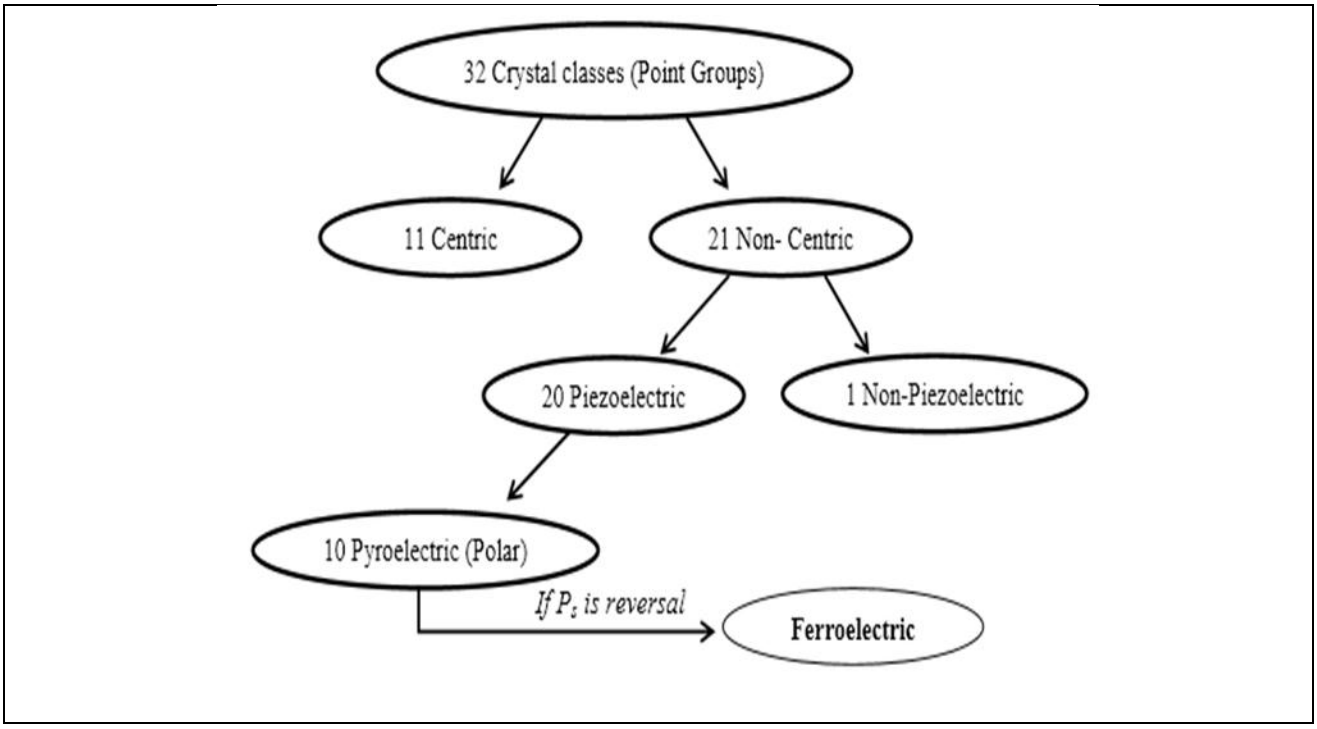


**Fig.2- A Classification scheme for the 32 crystallographic point groups**

## PIEZO ELECTRICITY

In certain crystals, the application of an external stress induces a net dipole moment which produces the electric polarization. Such crystals are called piezoelectric crystals and the phenomenon is called piezoelectricity. In these crystals the inverse effect is observed i.e. the application of an electric field produces strain in the crystal. Examples of such crystals: Quartz, Rochelle salt , Tourmaline etc .

In schematic one dimensional notation, the piezoelectric equations are :-

$$P=Z\,d+\varepsilon_0\,E\,\chi \qquad \text{——————} \qquad \text{(i)}$$

$$e=Z\,s+E\,d \qquad \text{——————} \qquad \text{(ii)}$$

where, P represents polarization, Z the stress, d the piezoelectric strain constant, E the electric field, $\chi$ the dielectric susceptibility, e the elastic strain and s the elastic compliance constant.

Equation (i) exhibits the development of polarization by an applied stress. And equation (ii) shows the development of elastic strain by applied electric field.

The absence of centre of inversion is the pre-requisite for the occurrence of piezoelectricity. Piezoelectric materials are used to convert electrical energy to mechanical energy and vice versa. They are used in devices such as Microphones, strain gauge, ultrasonic generators etc.

## PYROELECTRICITY

It is mentioned earlier that 10 out of 21 Non-centrosymmetry classes of materials show spontaneous polarization which response the temperature is called Pyroelectric effect.

$$\Delta P = \lambda \Delta T$$

Where,

**ΔP** = Spontaneous polarization

**λ** = Pyroelectric co-efficient

**ΔT** = Change in temperature

An increase in temperature leads to decrease in spontaneous polarization. Polarization suddenly falls to zero on heating above a particular temperature. This results thermal agitation with increase in temperature, leading to opposition of the dipoles to align in particular direction .

## INTRODUCTION TO BNT

It is being studied because of its high temperature dielectric constant, as well as its ability to work well without the addition of lead. Bismuth sodium titanate is an $ABO_3$ distorted perovskite with a rhombohedral crystal structure at room temperature. Bismuth sodium titanate is a relaxor ferroelectric in the rhombohedral phase and it exhibits diffuse phase transitions between each of the phases.

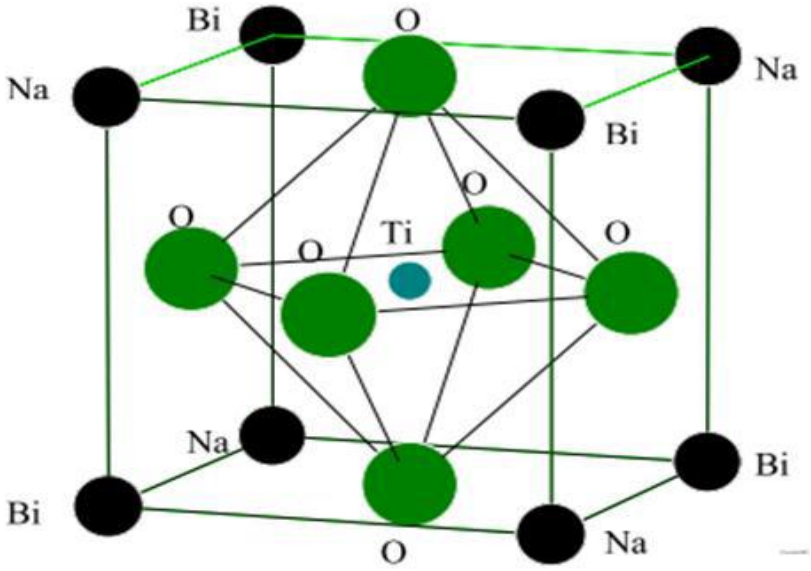


Fig.3- Representation of an $ABO_3$ perovskite shown as cubic BNT.

This figure shows that bismuth and sodium cations occupy the corners of a cubic unit cell, oxygen cations occupying the face centres, and a titanium cation in the center of the oxygen octahedra that is formed.

# CHAPTER 2

- THESIS OBJECTIVE

(A) To prepare the different compositions of BNT & LN by using the formula (1-x)BNT-x LN

(B) To study the effect of BNT due to the addition of different composition of LN by performing different characterization.

## 2.1 Literature review

The BNT material was discovered in 1960 by Smolenskiiet.al. In 1990, by various sources the optical and dielectric properties of BNT were reported by park et al., [1-3]. The existence of rhombohedral symmetry at room temperature was found out by Jones and Thomas in 2002. When heated, structural transition takes place from tetragonal to cubic .These BNT materials are having high Curie temperature. Doping is required to improve the properties of BNT materials. Some of the few examples of doping are –

Doping of Bi0.5 $Na_{0.5}TiO_3$ –$LiNbO_3$, Bi0.5 $Na_{0.5}TiO_3$-$CaTiO_3$, Bi0.5Na0.5TiO3- $BaTiO_3$, $Bi_{0.5}Na_{0.5}TiO_3$-$PbTiO_3$, Bi0.5Na0.5TiO3-$SrTiO_3$ and Bi0.5Na0.5TiO3 -$BiFeO_3$,
Bi0.Na 0.5 TiO3 -K0.5B0.5TiO3

Jiaming Li et al. investigated the addition of Fe and La on the dielectric, ferroelectric and the piezoelectric properties of (Bi0.5Na0.5)TiO3– Bi0.5Li0.5TiO3 – BaTiO3 Mn ceramics. A hard effect was created with a coercive field Ec of 2.9 kv/mm with the doping of Fe [4].While doping of La produced a soft effect with the improvement in piezoelectric constant with the decrease in coercive field.

Ferroelectric phase transitions are either displacive or order-disorder type. The displacive transition in perovskite ferroelectric (BaTiO3) occurs by the ionic displacement of B-site ion

within the oxygen octahedral cage. In an order-disorder ferroelectric, the randomly oriented dipole moment of unit cell points in the same direction within a domain upon lowering the temperature [5].

Nagata et al. reported on the properties of BNT by the addition of $BaTiO_3$ and BKT [6]. It was reported that at a composition containing 82.5% BNT,2.8% $BaTiO_3$ and 12% $Bi_{0.5}Na_{0.5}TiO_3$ morphotrophic phase boundary exists because of the anomalous electrical behavior associated with MPB compositions.

Man-Soon Yoon used the pre synthesized $BaTiO_3$ and pre milled bismuth oxide, sodium carbonate, and barium carbonate powders [7].The BNT – BT property was increased.

Jin Soo Kim et al synthesized BNT-LN ceramics in solid state reaction route[8]. They found with increasing $LiNbO_3$ doping, the dielectric constant peak at $T_m$=340$^oC$ shifted to low temperature and broadened, which was caused by an increase in the disorder at A and B sites. With increase in $LiNbO_3$doping, the P-E hysteresis loop to a linear relation characteristic of paraelectric phase.

H. Ni et al showed the preparation of BNBT–xKN (Bi0.5Na0.5TiO3–BaTiO3–KNbO3) ceramics by a conventional ceramic sintering technique and their piezoelectric, ferroelectric and dielectric performances have been investigated [9]. The results of XRD indicate that KN has diffused into the BNBT lattices to form a new solid solution with a pure perovskite structure, no phase transition is observed by adding KN into BNBT. Moderate introduction of KN into BNBT–xKN ceramic ($x \leq 0.02$) can enhance the properties like dielectric, piezoelectric and ferroelectric properties of BNBT–xKN.

K. Kumari et al prepared NBT-ZnO ceramics through a high-temperature solid-state reaction technique [10], have been found to have single-phase perovskite type rhombohedral structure. The addition of ZnO to NBT shifts *T*m to higher temperature side. A decrease in the value of

dielectric loss with increase in ZnO content has been observed, which is desirable for piezoelectric/ pyroelectric applications.

H.Nagata, T.Takenaka et al [11] studied the micro structure , dielectric , ferroelectric and piezoelectric properties of bismuth sodium titanate (Bi0.5Na0.5)TiO3 with MnCO3 doped. They found the curie temperature (Tc) decreases rapidly with increasing amount of doping. It is supposed that Mn ion mainly exist in the grain and substitute for A or B site of the perovskite structure. Also they found that the resistivity is anhanced to $3*10^{14}$ Ωcm.

M. Zannen et al showed the effect of Nd on BNT [12]. They observed a sharper dielectric transition with a lower dielectric peak value was obtained for NBT, but the ferroelectric properties were improved over pure BNT. The pyroelectric properties were also characterized, and a fairly high value of the pyroelectric coefficient was obtained.

# CHAPTER 3

This chapter includes the details about synthesis of BNT-LN ceramics and different experimental techniques used to characterize it.

## 3.1 EXPERIMENTAL TECHNIQUES

**(A)** Preparation of solid solution of BNT-LN by solid state reaction route.

**(B)** Characterization of the different compositions of BNT-LN ceramics.

## 3.2 SYNTHESIS METHODS

**(A)** Powder preparation

(B) Ball milling

(C) Powder calcination

(D) Pelletization

(E) Sintering of pellets

## 3.3 CHARACTERIZATION TECHNIQUES

**(A)** X-ray diffraction

**(B)** Raman Spectroscopy

**(C)** Scanning Electron Microscopy

**(D)** uv-visible Spectroscopy

**(E)** Dielectric study

**(F)** P-E loop

### 3.4 RAW MATERIALS USED FOR SYNTHESIS

**For BNT ($Bi_{0.5}Na_{0.5}TiO_3$) the row materials are**

$Bi_2O_3$ (Bismuth Oxide)

$Na_2CO_3$ (Sodium Carbonate)

$TiO_2$ (Titanium Oxide)

**For LN ($LiNbO_3$) the row materials are**

Li2CO3 (Lithium Carbonate)

Nb2O5 (Niobium pentoxide)

### 3.5 PREPARATION OF POWDER (BNT AND LiNbO3) BY SOLID STATE

**SYNTHESIS ROUTE**

Solid state synthesis route is adopted due to its easiness and the precursors used are less expensive. The raw materials are weighed in stoichiometric proportion to start the synthesis process.

The chemical equation of Sodium bismuth titanate(BNT) is

$$Na_2CO_3 + Bi_2O_3 + 4\,TiO_2 \longrightarrow 4Bi_{0.5}Na_{0.5}TiO_3 + CO_2 \uparrow$$

The chemical equation of lithium niobate (LN)is

$$Li_2CO_3 + Nb_2O_5 \longrightarrow 2LiNbO_3 + CO_2 \uparrow$$

### 3.6 FLOW CHART OF WORK

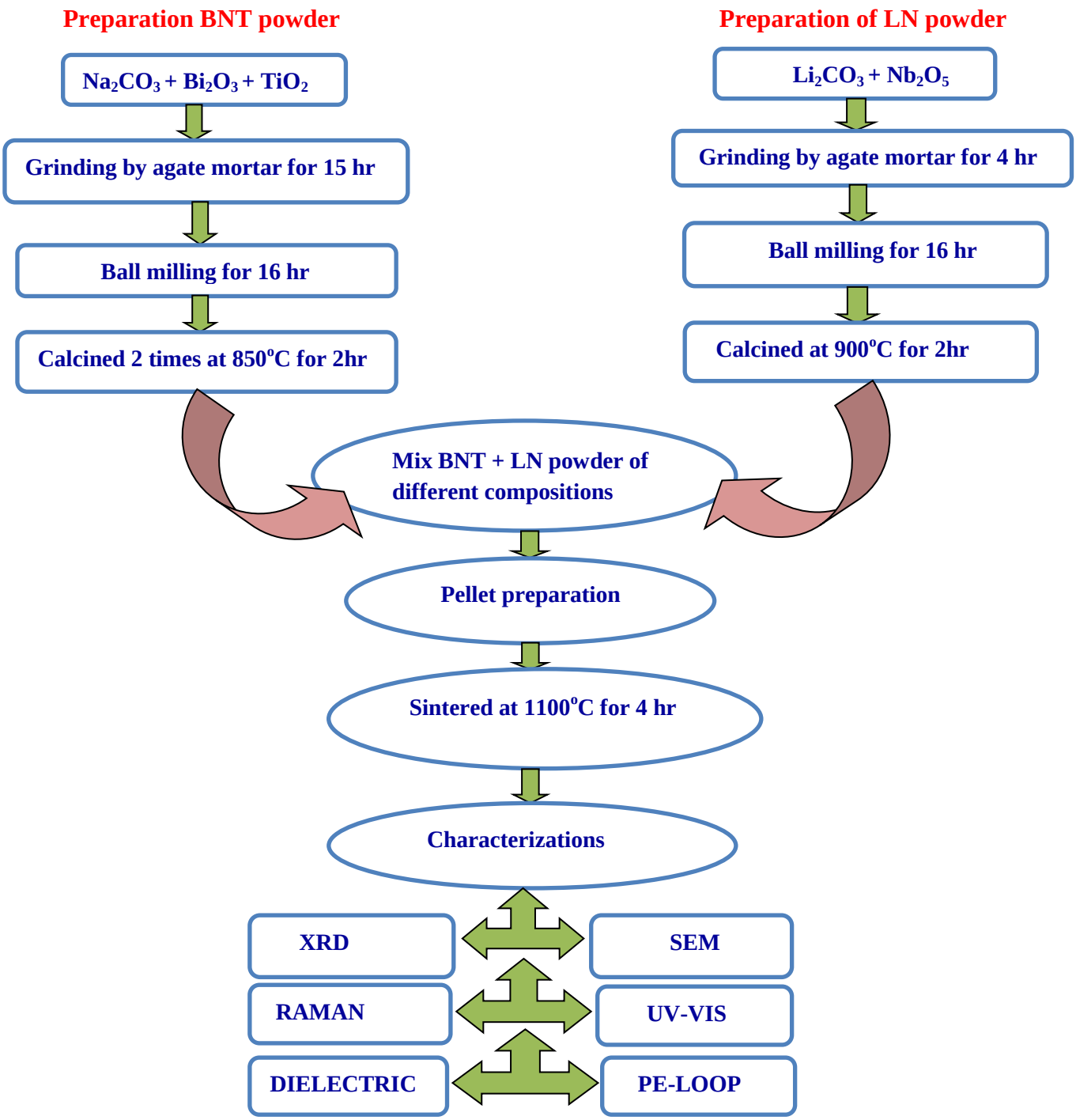

## 3.7 EXPLANATION OF DIFFERENT PROSESSES USED IN SYNTHESIS

### Ball milling

The BNT, LN powder were ball milled separately for sixteen hours using zirconia balls and acetone as a medium then it left for drying , then the balls and powder are separated out. By ball milling the materials are grinded to fine powder.

### Calcination

It is the heat treatment process in which solid state reaction takes place between the constituent particles results phase formation. Here the pure BNT is calcined two times at $850^{o}C$ for two hours for better phase formation. And the Lithium niobate ($LiNbO_3$) is calcined at $900^{o}C$ for two hours.

### Mixing different compositions of BNT with LN

BNT-LN compositions were made by using the formula (1-x) BNT-x LN with different weight fractions of LN taking x=0.02, 0.04, 0.06, 0.08, 0.10

### Pellet formation

The calcined powders of different compositions mixed by PVA binder and grinded for four hours continuously. After drying the sample is scrapped out from the agate mortar and separately pellets are prepared by the help of dieset and pelletize under a load of 5 ton.

### Sintering

The prepared pellets were sintered at $1100^{o}C$ in a furnace for four hours. Sintering is done to densify the pellets and to make compact. The sintering also causes the diffusion of atoms which will help in grain growth and the decrease in porosity is also observed. The type of

furnace used is an electrically heated one. To get good result it is necessary to control the heating rate and temperature.

## 3.8 EXPLANATION OF DIFFERENT CHARACTERIZATION TECHNIQUES

### X-ray diffraction (XRD)

X-rays are electromagnetic radiations having shorter wavelength than that of visible light. X-ray diffractometer based on the principle of Bragg's law which is given by

$$2d\sin\theta = n\lambda$$

Where, d is the spacing between the atomic planes,

$\lambda$ is the wavelength of x-ray used

$\theta$ is the angle of diffraction.

And n =1, 2, 3

The x-ray diffraction is a technique for determination of different phases present in the sample, crystal structure and the crystallite size.

The pellets of different compositions of sodium bismuth titanate and Lithium niobate were subjected to x-ray diffraction and the results were obtained.

### Scanning Electron microscopy (SEM)

In SEM when a beam of high energetic electrons strikes the sample the x rays, secondary electrons, and back-scattered electrons are produced from the sample. The detector then collects these electrons and converted into signal and displays on the screen. Since the samples are non-conducting, so a thin layer of platinum is coated using a sputter coater. Generally SEM provides the information about the surface of the specimen and it can't scan

deep into the surface. In SEM the electrons beam are focused on small area of the sample. This characterization technique provides the information about the surface morphology of the sintered pellets.

**Dielectric Study**

For dielectric measurement the impedance analyzer was used. The data containing phase, impedance, capacitance and conductance are collected as a function of frequencies at different temperatures.

**Raman Spectroscopy Study**

Raman spectroscopy is a technique by which we can analyze the vibrational and rotational modes in a system. The frequencies of spectral line are greater or less than the original frequencies. The frequency in raman lines are not determined by the scattered but by the incident frequency.

**CHAPTER 4**

# RESULT AND DISCUSSION

## 1. XRD Analysis

Fig. 1 shows the XRD patterns of (1-*x*)BNT-*x*LN ceramics with various *x* values at room temperature. The XRD peaks of the BNT and the BNT-LN ceramics were in agreement with those of the previous BNT phase with the $ABO_3$ perovskite structure. This indicated that BNT-LN single phases were formed at different $LiNbO_3$ doping, and no second peaks were observed. Thus, the BNT-LN ceramics, as well as the BNT ceramics, had a rhombohedral system. The position of peaks shifted towards lower angle at higher concentration of LN may be due to sudden rise of strain in the material by the solubility limit of LN in the BNT lattice were reached.

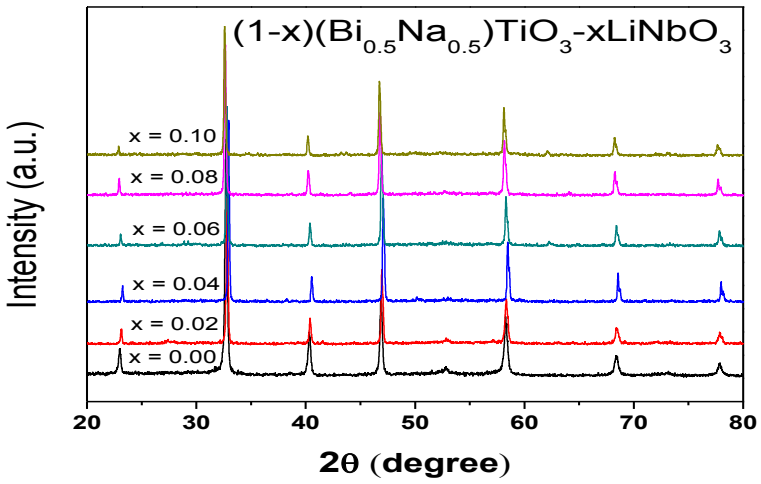


Fig.4-XRD patterns of (1-*x*)BNT-*x*LN solid solution ceramics

## 2. Raman Spectroscopy Analysis

As per the Group theory analysis, BNT (rhombohedral, R3c) should show 13 Raman active modes; in irreducible representation $\Gamma_{Raman} = 7A_1 + 6E$. Therefore, among the 13 Raman-active vibrational modes it is possible to observe 8 Raman-active from fitting deconvolution of the Raman spectrum of BNT and all the compositions of BNT-LN ceramics (only Lorentzian Area function). This can be attributed to A-site and B-site disorder and the overlapping of Raman modes due to the lattice anharmonicity. The Raman patterns shows roughness or irregularity due to the data taken in high resolution, it makes noise while collections of data. If we take the data in low resolution, then it is impossible to distinguish the closely bounded molecules.

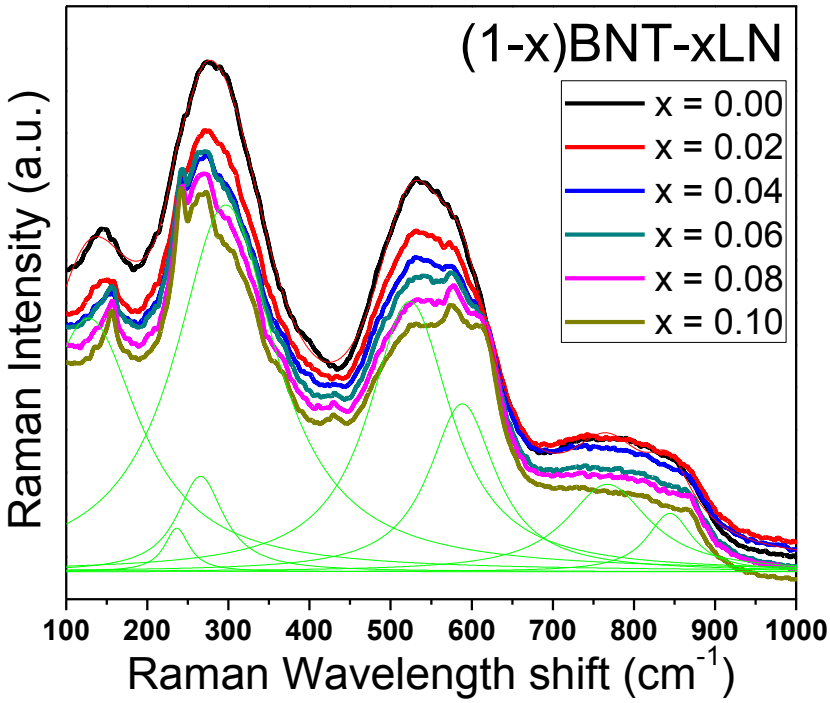


Fig.5- Room temperature Raman spectra of (1-*x*)BNT-*x*LN solid solution ceramics

## 3. Scanning Electron Microscopy Analysis

Fig.3 shows SEM images of the pure BNT and the BNT-LN ceramics. The grains were well developed at sintering temperatures of 1075 - 1150$^{o}$C for 4 h. The grains of the BNT ceramics had a dense structure, which were similar to those of a typical BNT ceramics. With increasing $LiNbO_3$, the grain shape changed from granular-like grains for BNT to plated grains plated grains for the BNT-LN ceramics. Grain growth is slightly inhibited after $LiNbO_3$ doping for the (1-*x*)($Bi_{0.5}Na_{0.5}$)$TiO_3$-*x*$LiNbO_3$ ceramic systems and thus non-uniform grains are formed.

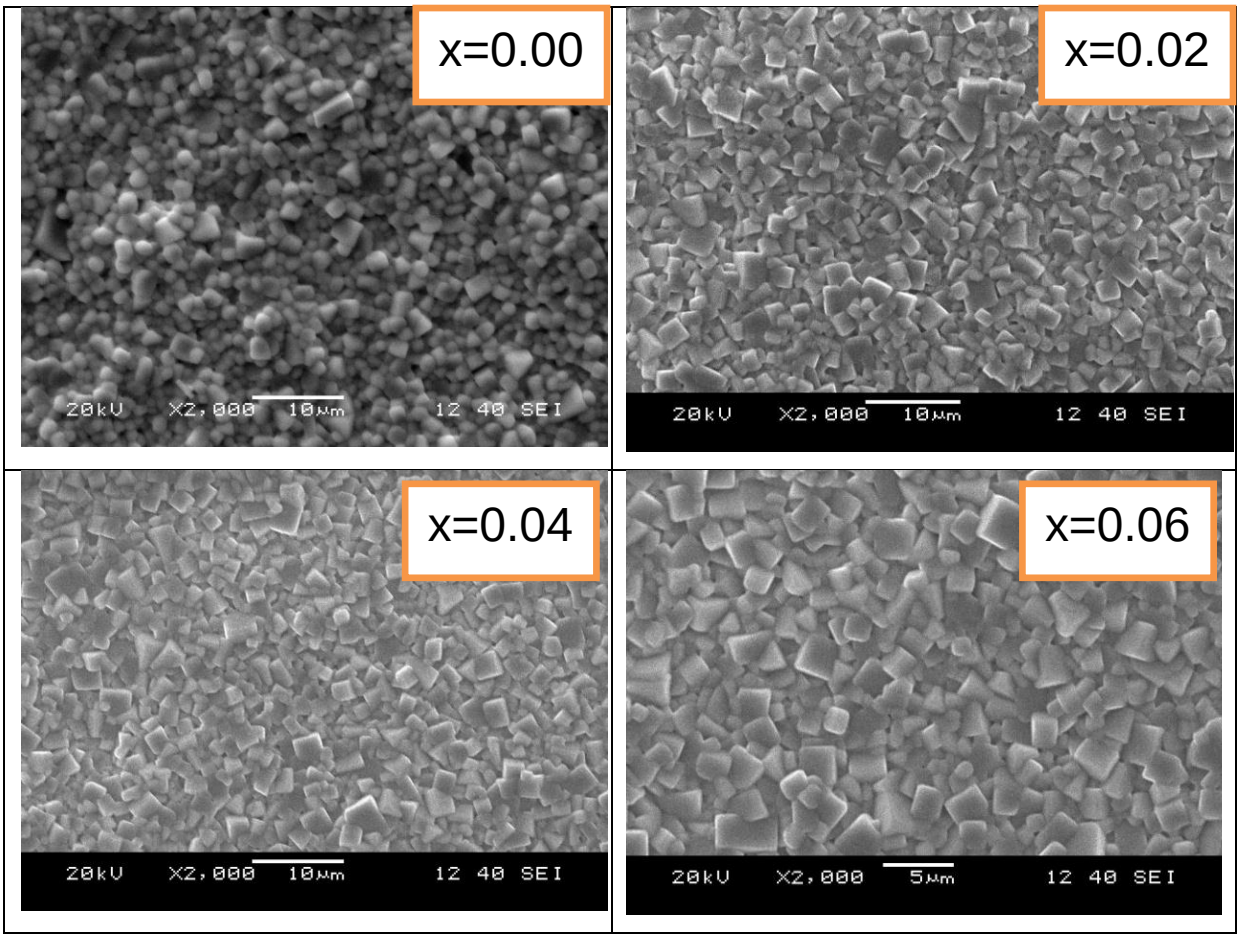

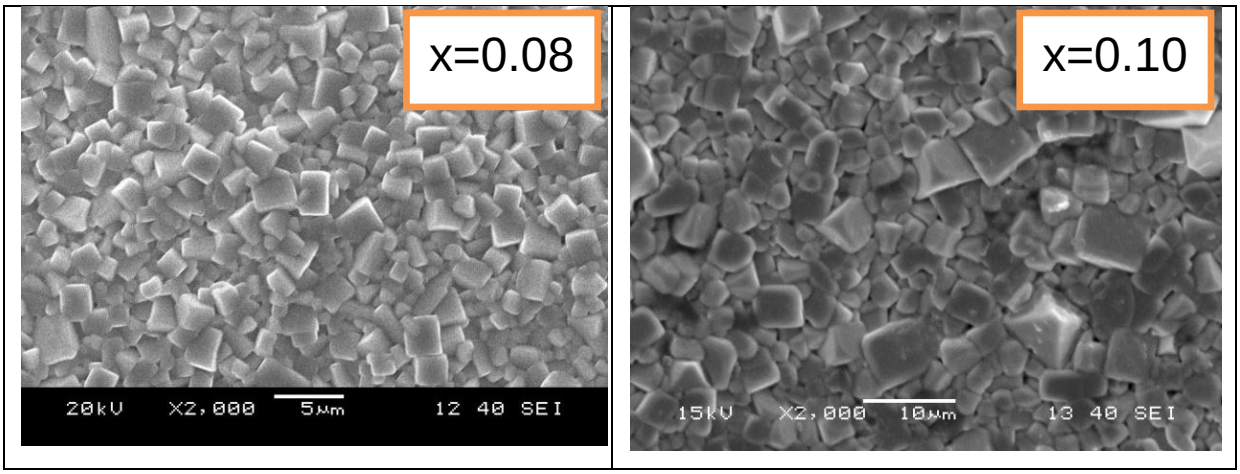


Fig.6- Scanning electron microscopy (SEM) of (1-*x*)BNT-*x*LN solid solution ceramics

## 4. UV Visible Spectroscopy Analysis

The optical band gap energy ($E_{gap}$) was estimated for BNT-LN ceramics by using the method proposed by Wood and Tauc and presented in fig 7. According to these authors the optical band gap is associated with the absorbance and photon energy by the following equation:

$$h\nu\alpha \propto (h\nu - E_{gap})^n$$

where h is the Planck constant, α is the absorbance, ν is the frequency, $E_{gap}$ is the optical band gap and n is a constant associated to the different types of electronic transitions (n = 0.5, 2, 1.5 or 3 for direct allowed, indirect allowed, direct forbidden and indirect forbidden transitions, respectively). In our work, the UV-visible absorbance spectra indicated an indirect allowed transition and, therefore, the value of n = 2 are used in the above equation. The literature describes that the band gap energy is indirect when the electronic transitions occur from maximum-energy states located near or in the valence band (VB) to minimum-energy states below or in the conduction band (CB), but in different regions in the Brillouin zone. Thus, the $E_{gap}$ value for BNT-LN powders was evaluated extrapolating the linear portion of the curve or tail. The enhanced optical band gap is observed with the increase in LN content in BNT-LN ceramics in the studied composition range.

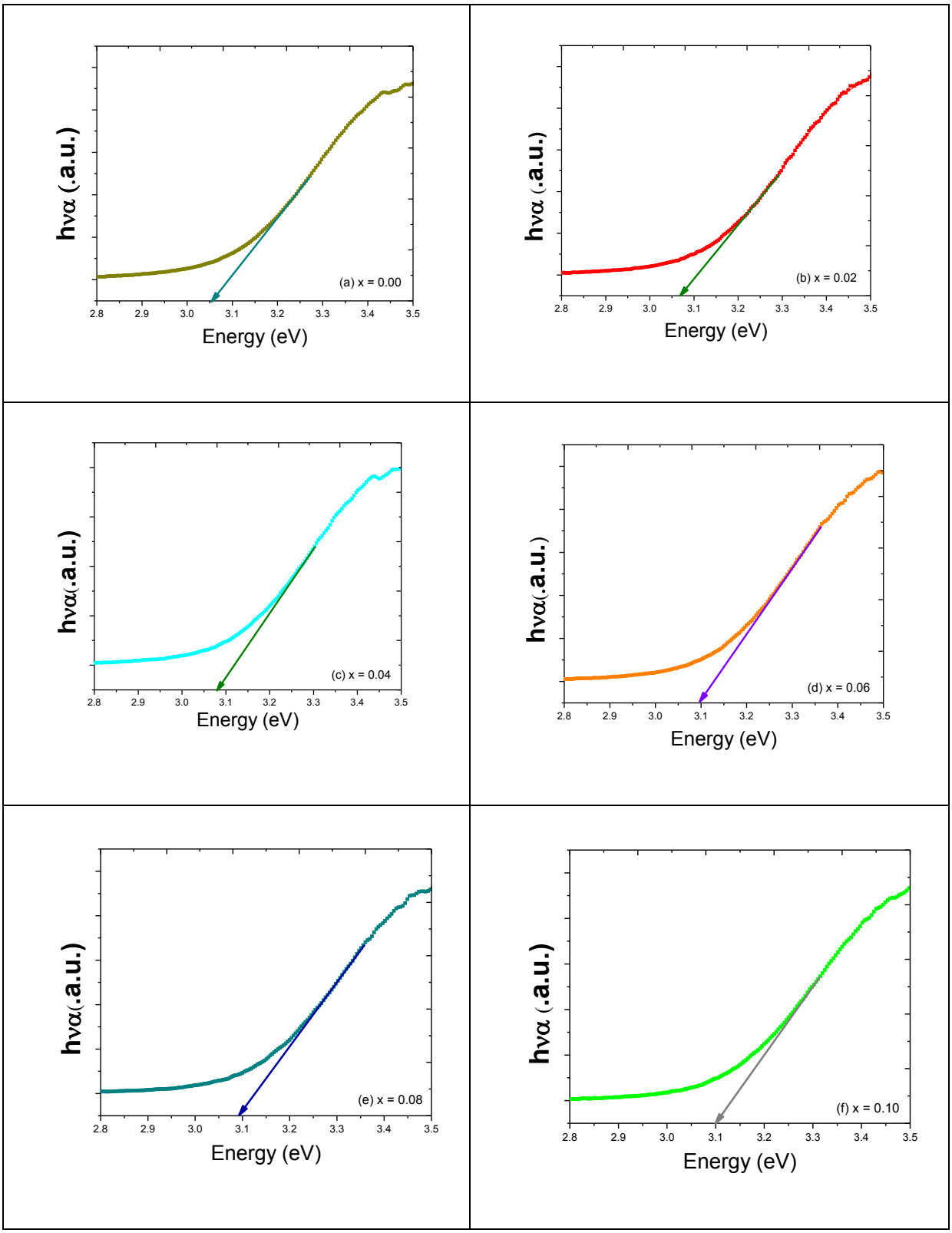


Fig.7- The optical band gap calculated by extrapolating the linear portion of the absorption spectra for (1-*x*)BNT-*x*LN ceramics.

In principle, this behaviour indicates the existence of different intermediary energy levels within the band gap of these materials, which can be arising from the structural order–disorder into the lattice. Thus, the increase of LN content is able to induce a structural rearrangement, reducing the presence of these energy levels within the band gap and increasing the $E_{gap}$ values. Based on this hypothesis, we believe that the intermediary energy levels are composed of deep and shallow holes.

## 5. PE-LOOP

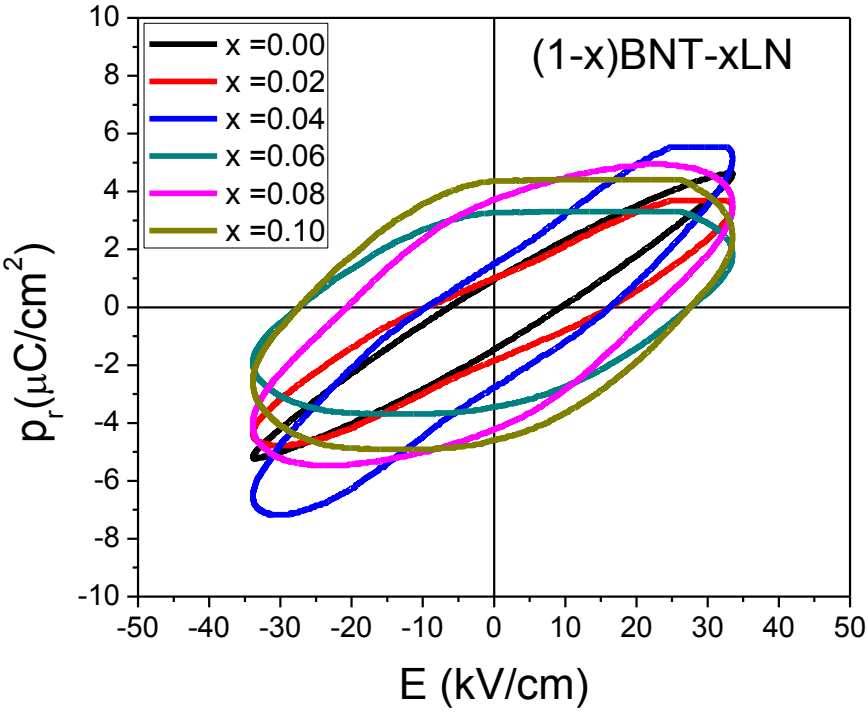


Fig.8- Ferroelectric P-E hysteresis loops of the BNT and the BNT:LN ceramics.

Figure 8 shows the P-E hysteresis loops of the BNT and the BNT:LN ceramics at room temperature. It can be seen that typical ferroelectric polarization hysteresis loops were

obtained for all samples under an electric field of 35 kV/cm at15Hz. It is found that the LN content has an effect on the ferroelectric properties of the ceramics. It can be seen that the Pr and Ec values generally increases with increasing the LN content. P-E loops looks not very slim probably because of slightly high leakage currents as can be seen from the round angle of the P-E loops at the maximum electric field and at the higher concentration of LN content.

## DIELECTRIC STUDY

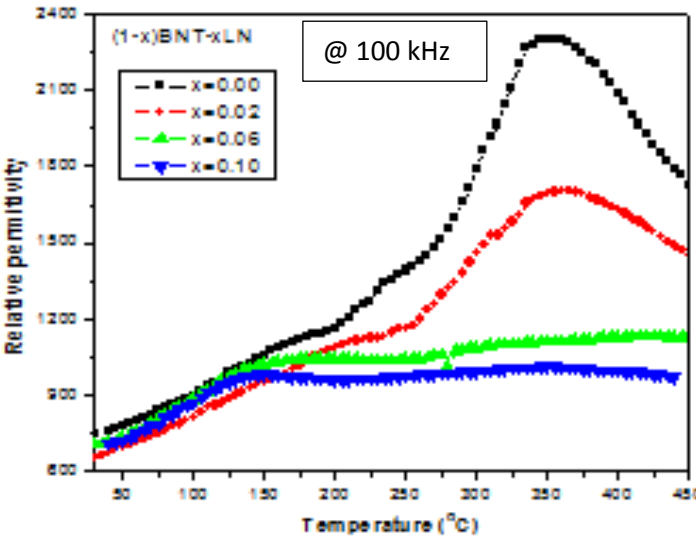


Fig.9- Dielectric constant of the BNT and the BNT-LN Ceramic system.

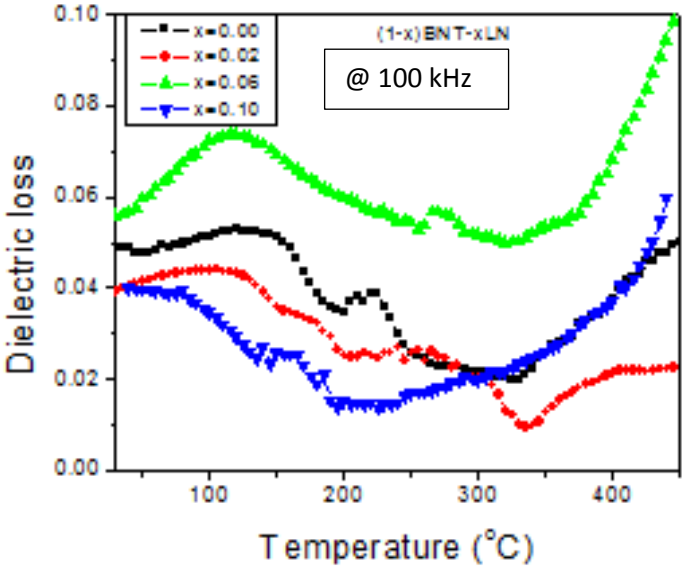


Fig.10- dielectric loss of BNT and BNT- . LN Ceramic system.

Fig. 9 shows the temperature dependence of relative permittivity at a frequency of 100 kHz. There are two dielectric peaks for the BNT ceramic [13-18]. The first peak in around 200°C is the depolarization temperature ($T_d$), which is similar to that of the phase transition from the ferroelectric to the antiferroelectric phase. The second peak is a phase transition to the paraelectric phase. The variations in the dielectric behaviors are at tributed to the increased $LiNbO_3$ doping. With increasing $LiNbO_3$ doping, the dielectric peak near $T_m$ = 350°C broadened and shifted to low temperature. The dielectric properties with a broad dielectric maximum are reported to be due to the contribution of a relaxor behavior, which is called a diffuse phase transition (DPT). In this work, $LiNbO_3$ doping caused an inhomogeneous

composition and a more disordered crystal structure,That results the broad dielectric maximum. Thus, the diffuse phase transition could be explained by the coexistence of a (Na, Bi, Li) ion at the A-site and a (Ti, Nb) ion at the B-site.

Fig. 10 shows the temperature dependence of dielectric loss (tanδ) at a frequency of 100 kHz. With increasing temperature, the dielectric constant of the BNT ceramics decreased up to a temperature of 300$^{o}$C and then increased due to bismuth and oxygen vacancies are created at high sintering temperatures, which cause the strong low frequency dielectric dispersion and high electrical conductivity. The defects get trapped at sites like grain boundaries and grain-electrode interfaces and results space charge polarization so electrical conductivity increases. The decrease in the dielectric constant indicated that the electrical conductivity decreased. This implies that $LiNbO_3$ doping reduces the contribution of space charge or ionic charge carriers.

# CHAPTER – 5

## Conclusion

- Single phase Perovskite BNT, LN and (1-x)BNT-xCT ceramic successfully prepare through solid state reaction route.

- XRD patterns indicating that the position of peaks shifted towards lower angle at higher concentration of LN may be due to sudden rise of strain in the material.

- The Raman patterns shows roughness or irregularity due to the data taken in high resolution.

- SEM images shows that with increasing the LN concentration the grain growth slightly inhibited and the grain shape changed from granular to plate shaped.

- UV plot shows that the band gap increases with increase in LN concentration.

- PE loop shows that the remnant polarization(Pr) and coercive field(Ec) increasing with increase in LN concentration.

- Dielectric study shows that with increasing $LiNbO_3$ doping, the dielectric peak near $T_m = 350^oC$ broadened and shifted to low temperature and the dielectric loss study shows the conductivity reduced due to increase in LN concentration.

## REFERENCES-

1. J.A. Zvirgzds, P.P. Kapostins, J.V. Zvirgzde, and T.V. Krunjina, "X-ray studies of phase Transition in ferroelectric Na0.5Bi0.5TiO3," Ferroelectrics, 40[1-2] 75-7 (1982).

2. S.-E. Park and K.S. Hong , "Variation of structure and dielectric properties on substituting cations for Sr2+ in (Bi1/2Na1/2) TiO3, "J.Mater. Res., 12 [8] 2152-7 (1997).

3. K.Sakata and Y.Masuda, Ferroelectrics, 7 [1-4] 347-9 (1974).

4. JiamingLi .Feifei Wang .Chung Ming Leung. Siu Wing or .YanxueTang .Xinman Chen. Tao Wang .XiaomeiQin .Wangzhou Shi. DOI 10.1007/s10853-011-5523-7

5. W. Chen, W. Zhu, O. K. Tan and X. F. Chen, Frequency and temperature dependent impedance spectroscopy of cobalt ferrite composite thick films. Journal of applied physics, 108 (2010) 034101.

6. H.Nagata, M.Yoshida, Y.makiuchi and T.Takenaka,,Jpn. J. Appl. Phys., 42[12] 7401- 3 (2003)

7. Man –Soon Yoon , NeamulHayetKhansur , Byung –Ki Choi , Young – Geun Lee , Soon Chul Ur Ceramics International 35 (2009) 3027 – 3036.

8. Journal of the Korean physical society , Vol. 58, No. 3, March 2011 , pp. 659~662.

9. Journal of Alloys and Compounds *509 (2011) 3958–3962*

10. J. Mater. Sci. Technol., 2011, **27**(3), 213–217

11. Journal of the European ceramic society 21 (2001) 1299-1302

12. Materials Chemistry and Physics 134 (2012) 829-833

13. T. Oh, Jpn. J. Appl. Phys. 45, 5138 (2006).

14. J. S. Kim, J. H. Jeong, S. Y. Cho, M. S. Jang and S. B. Cho, J. Korean Phys. Soc. 51, 137 (2007).

15. J. S. Kim, S. Y. Cho and M. S. Jang, J. Korean Phys. Soc. 51, 692 (2007).

16. G. Fan, W. Lu, X. Wang, F. Liang and J. Xiao, J. Phys. D: Appl. Phys. 41, 035403 (2008).

17. W. Jo, T. Granzow, E. Aulbach, J. Rodel and D. Damjanovic, J. Appl. Phys. 105, 094102 (2009).

18. T. K. Song, M.-H. Kim, Y.-S. Sung, H. G. Yeo, S. H. Lee, S.-J. Jeong and J.-S. Song, J. Korean Phys. Soc. 51, 697 (2007).